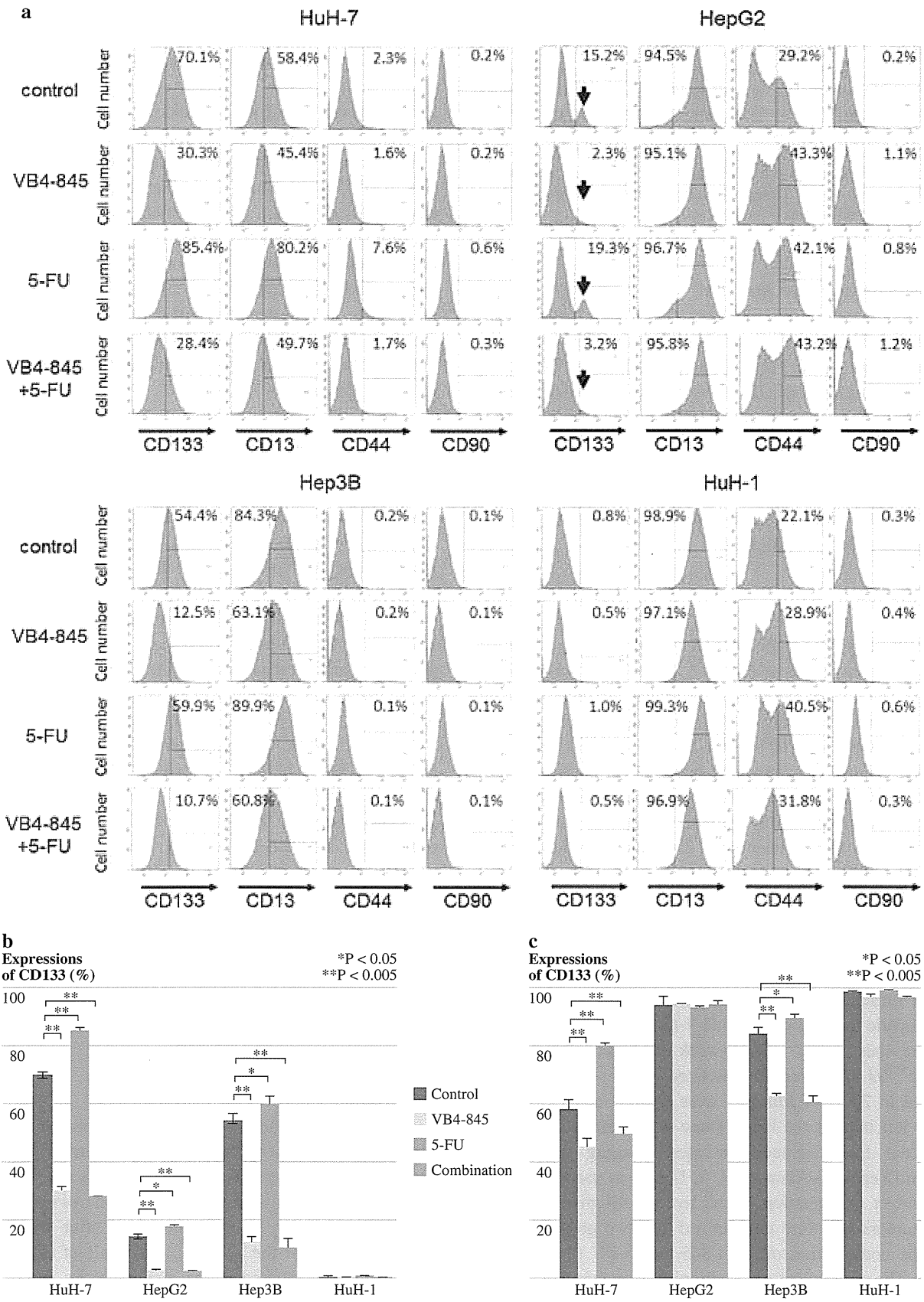
a
HuH-7
HepG2
Hep3B
HuH-1
control
VB4-845
5-FU
VB4-845 +5-FU
Cell number
70.1%
58.4%
2.3%
0.2%
15.2%
94.5%
29.2%
0.2%
30.3%
45.4%
1.6%
0.2%
2.3%
95.1%
43.3%
1.1%
85.4%
80.2%
7.6%
0.6%
19.3%
96.7%
42.1%
0.8%
28.4%
49.7%
1.7%
0.3%
3.2%
95.8%
43.2%
1.2%
54.4%
84.3%
0.2%
0.1%
0.8%
98.9%
22.1%
0.3%
12.5%
63.1%
0.2%
0.1%
0.5%
97.1%
28.9%
0.4%
59.9%
89.9%
0.1%
0.1%
1.0%
99.3%
40.5%
0.6%
10.7%
60.8%
0.1%
0.1%
0.5%
96.9%
31.8%
0.3%
CD133
CD13
CD44
CD90
b
Expressions of CD133 (%)
*P < 0.05
**P < 0.005
Control
VB4-845
5-FU
Combination
HuH-7
HepG2
Hep3B
HuH-1
c
Expressions of CD133 (%)
*P < 0.05
**P < 0.005
HuH-7
HepG2
Hep3B
HuH-1

◀**FIG. 3** FACS analysis of EpCAM^{high} cell lines based on various stem/progenitor markers after the treatment of VB4-845 (1 pM), 5-FU (5 μg/ml), and the combination of VB4-845 plus 5-FU. **a** A representative result of three independent staining experiments is shown and the positive rate of markers corresponding to the graph was indicated. *Arrow* shows a unique bimodal pattern of HepG2 cells for CD133 expression. **b** Expression of CD133 after the treatment of VB4-845 and/or 5-FU. *Columns*, CD133 positive cells (%); *vertical bars*, standard deviation. **c** Expression of CD13 after the treatment of VB4-845 and/or 5-FU. *Columns*, CD13 positive cells (%); *vertical bars*, standard deviation

Immunohistochemical Analysis

Immunohistochemical analysis of EpCAM was performed using #ab71916 (Abcam, Cambridge, UK) using Ventana (Tucson, AZ, USA) as previously described.[17,26] The tumor cells showed equivalent membranous staining to normal bile duct epithelium was defined as strongly stained tumor cells. The immunostaining was evaluated quantitatively by counting in no fewer than three different random fields (100× magnification) under a light microscope by two independent investigators.

In Vivo Studies

A subcutaneous tumor model was created as described in our previous reports.[23,24,26,27] Twenty-five-week-old female NOD.CB17-PRkdc^{Scid}/J mice purchased from Charles River Laboratory Inc. (Kanagawa, Japan) were injected with 1×10^6 HuH-7 cells mixed half with Matrigel (BD Biosciences) subcutaneously into the both flanks under anesthesia and 16 mice were injected with 1×10^6 SK-Hep1 cells as well. Palpable tumors were confirmed in all injection sites 2 weeks after the inoculation, and mice were randomized into four groups: control, VB4-845 (30 μg/kg), 5-FU (30 mg/kg), and a combination of VB4-845 and 5-FU. VB4-845 diluted in 100 μl of saline was administered by tail vein injection, and/or 5-FU was injected intraperitoneally three times a week for 2 weeks.

An orthotopic xenograft model was created by direct intrahepatic inoculation of HuH-7-*Luc* cells, as described in our previous report.[23] Ten 5-week-old female NOD.CB17-PRkdc^{Scid}/J mice were anesthetized and 5×10^5 cells suspended in 20 μl of Matrigel were slowly injected into the upper left lobe of the liver. Three weeks after the inoculation, the luciferase-luciferin-based imaging using IVIS system (Xenogen, Alameda, CA, USa) was used to monitor the correct implantation in the liver.[28] All mice exhibited liver tumors and were randomized into two groups; control and the combination of VB4-845 and 5-FU (five mice in each). The protocol of drug administration was same as the subcutaneous model. All in vivo procedures were approved by the Animal Care Committee (permission #0130059A).

RESULTS

Expression of EpCAM in Human HCC Cells

The expression of EpCAM protein was assessed using FACS analysis in eight human HCC cell lines (Fig. 1a). These cell lines were divided into two groups: EpCAM high-expression (EpCAM^{high}) cell lines, including HuH-7 (98 ± 0.3 %), HepG2 (98 ± 0.9 %), Hep3B (99.8 ± 0.1 %), and HuH-1 (97.7 ± 0.2 %) in which more than 95 % of cells were positive for EpCAM; and EpCAM low-expression (EpCAM^{low}) cell lines, including HLE (0.4 ± 0.1 %), HLF (0.4 ± 0.2 %), PLC/PRF/5 (4 ± 0.3 %), and SK-Hep1 (0.7 ± 0.2 %) in which less than 5 % of cells were positive for EpCAM. The expression level of EpCAM in each cell line was confirmed immunocytochemically (Supplementary Fig. 1).

In Vitro Effects of VB4-845 and/or 5-FU

VB4-845, an immunotoxin targeting EpCAM,[20] was effective for EpCAM^{high} cell lines but not for the EpCAM^{low} cell lines (Fig. 1b). The IC_{50} value of VB4-845 was $4.6 \pm 0.1 \times 10^{-2}$ pM for HuH-7, $1 \pm 0.1 \times 10^{-2}$ pM for HepG2, $0.9 \pm 0.1 \times 10^{-2}$ pM for Hep3B, and $7.3 \pm 0.2 \times 10^{-2}$ pM for HuH-1. On the other hand, VB4-845 had no effect against EpCAM^{low} cell lines at all. 5-FU showed potent antiproliferative activity in all HCC cell types with IC_{50} value of 0.8 ± 0.1 μg/ml for HuH-7, 39.5 ± 9.6 μg/ml for HepG2, 5.9 ± 1.8 μg/ml for Hep3B, 11.3 ± 6.3 μg/ml for HuH-1, 16.5 ± 6.6 μg/ml for HLE, 33.5 ± 17.2 μg/ml for HLF, 55.6 ± 11.2 μg/ml for PLC/PRF/5, 4.3 ± 0.5 μg/ml for SK-Hep1 cells (Fig. 1c). There was no significant correlation between the efficacy of 5-FU and the expression of EpCAM in each cell line ($R = 0.16$, $p = 0.38$).

The combination effects of VB4-845 and 5-FU were assessed in eight human HCC cell lines (Fig. 1d). The combination of VB4-845 and 5-FU significantly suppressed cell proliferation in all of the EpCAM^{high} cell lines ($p < 0.05$). However, the EpCAM^{low} cell lines did not demonstrate the combined effects of both drugs. Therefore, the EpCAM^{high} cell lines were chosen for further analysis.

Sphere Formation Assay

After the treatment with VB4-845 and/or 5-FU on EpCAM^{high} cell lines, the viable cells were collected and analyzed for their ability to form spheres on reculturing (Fig. 2a). After 7 days, the number of spheres (>100 μm in diameter) was significantly decreased after exposure to VB4-845 alone or the combination in all of the four cell lines, but not altered after exposure to 5-FU alone (Fig. 2b). Although the doses of VB4-845 and 5-FU used in this assay showed similar antiproliferative activity

(Fig. 1d), their effects on sphere-forming ability were in direct opposition to one another. Because the sphere-forming cells are assumed to be capable of self-renewal, one of essential hallmarks of stemness, the effect of VB4-845 for EpCAM^{high} cell lines was found to be closely associated with their stemness.[25,29]

Alterations of Stem/Progenitor Markers

In the EpCAM^{high} cell lines, we analyzed the expression of several stem/progenitor markers, such as CD133, CD13, CD44, and CD90, using FACS analysis after the treatment of VB4-845 and/or 5-FU (Fig. 3a). These markers were chosen, because they were reported as biomarkers of HCC with poor prognosis.[7–10] The positive rate of CD133 was significantly decreased with the treatment of VB4-845 or combination, but increased with the treatment of 5-FU (Fig. 3b; $p < 0.05$). Interestingly, HepG2 cells showed a unique bimodal pattern for CD133 expression (Fig. 3a, arrow) and VB4-845 dramatically decreased this CD133-positive subpopulation of HepG2 cells with statistical significance. The positive rate of CD13 was significantly decreased with VB4-845, but increased with 5-FU treatment in HuH-7 and Hep3B cells (Fig. 3c, $p < 0.05$). There was no consistent tendency for the positive rate of CD44 and CD90 after the treatment of each cell line. Our results might indicate the effect of VB4-845 might be closely associated with the stemness of human HCC cells.

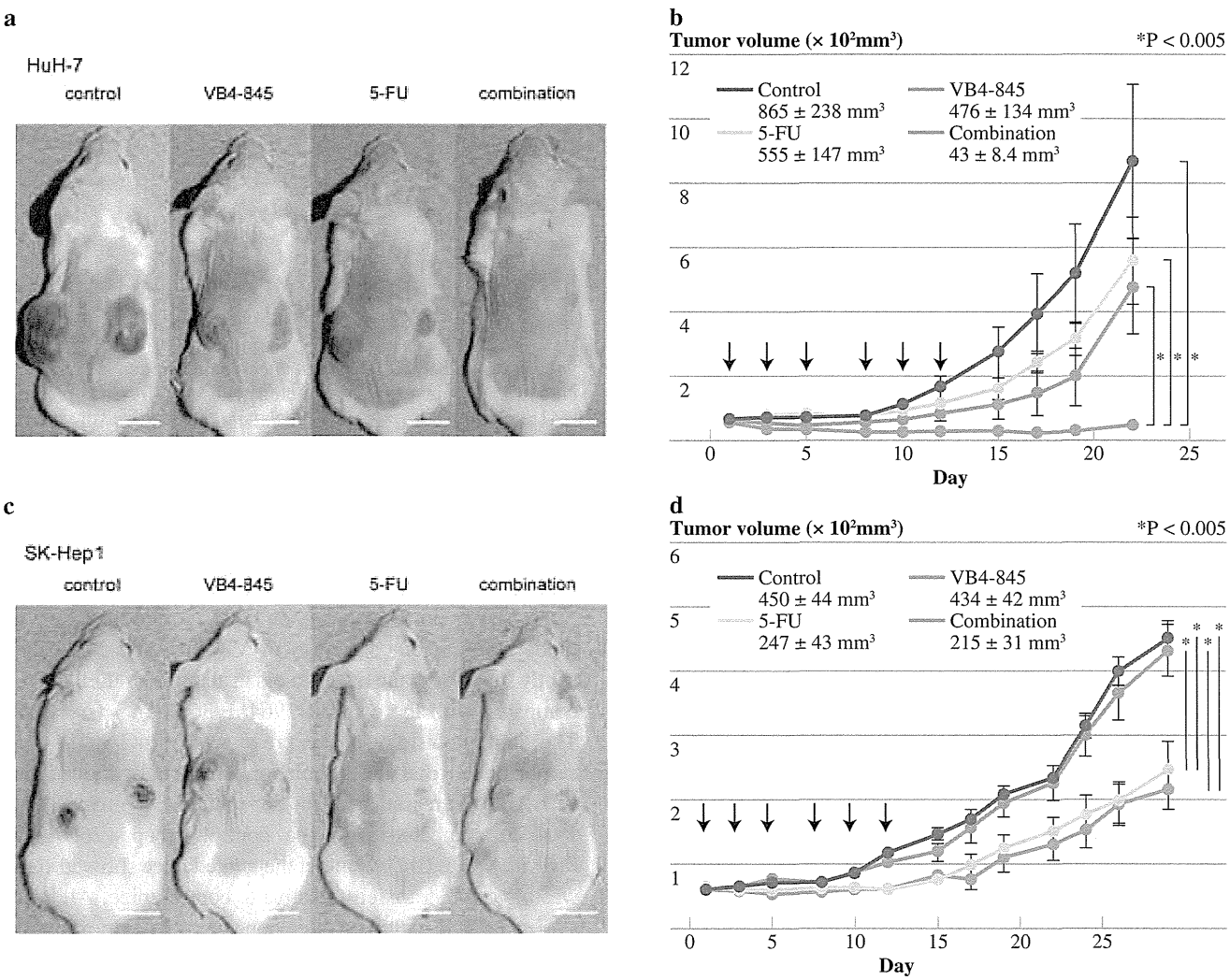

FIG. 4 In vivo studies in subcutaneous xenograft models using HuH-7 EpCAM^{high} or SK-Hep1 EpCAM^{low} HCC cells. Established subcutaneous xenografts derived from HuH-7 (**a**, **b**) or SK-Hep1 (**c**, **d**) were treated with intravenous injection of control saline or VB4-845 (30 μg/kg) and intraperitoneal injection of control saline or 5-FU (30 mg/kg) three times per week for 2 weeks. **a**, **c** Representative subcutaneous tumors in mice at the end of the dosing period. *Scale bar*, 10 mm. **b**, **d** Tumor size were measured using calipers three times a week in the four groups, and volumes were calculated using the following equation: volume = (length) × (width)^2 × 0.5. *Arrows* indicate the time of administration. *Vertical bars*, standard error. Statistical analysis was done by two-tailed Student's *t* test ($p < 0.05$)

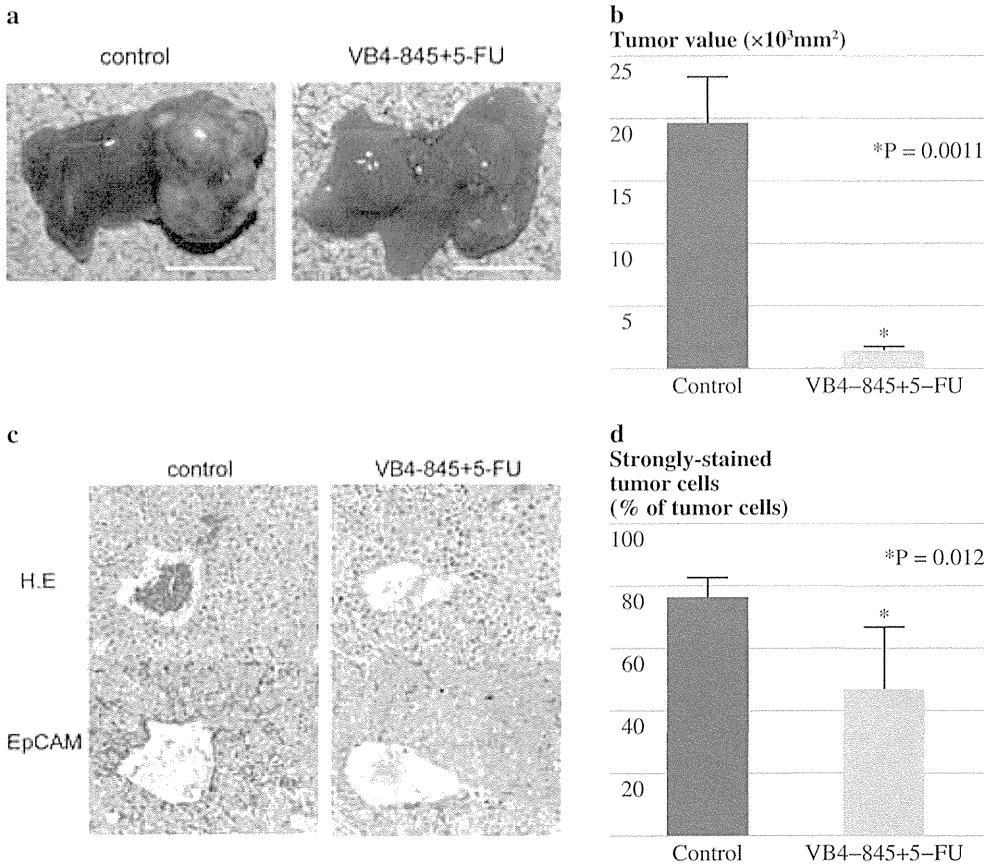

FIG. 5 In vivo studies in liver orthotopic xenograft models. Established liver orthotopic xenografts of HuH-7 were treated with control saline or the combination of VB4-845 plus 5-FU. The method and schedule of administration was the same as the subcutaneous tumor. Two weeks after the initiation of treatment, mice were sacrificed and the size of liver tumor was measured. **a** Representative liver tumor in mice at the end of the dosing period. *Scale bar*, 10 mm. **b** Liver tumor volume was analyzed 2 weeks after administration of the control (1964 ± 367 mm^3) or the combination of VB4-845 plus 5-FU (141 ± 34 mm^3) ($n = 5$). *Vertical bars*, standard error. Statistical analysis was done by two-tailed Student's t test ($p = 0.0011$). **c** H&E staining and immunostaining of EpCAM (magnification, ×40). **d** The percentage of strongly stained tumor cells in all of tumor cells between two groups. *Vertical bars*, standard deviation

In Vivo Effects of VB4-845 and/or 5-FU

To investigate in vivo antitumor activity, NOD.CB17-PRkdc^{Scid}/J mice bearing established HuH-7 (EpCAM^{high}) and SK-Hep1 (EpCAM^{low}) subcutaneous xenografts were utilized. In HuH-7 xenograft model, the volume of the tumors in the VB4-845 and 5-FU monotherapy groups appeared smaller, albeit not significantly, compared with the control group ($p = 0.078$ and 0.31, respectively, Figs. 4a, b). It is noteworthy that significant tumor regression was observed in the group treated with VB4-845 plus 5-FU compared with either the control or monotherapy groups ($p < 0.005$). On the other hand, any antitumor effect was not observed in SK-Hep1 EpCAM^{low} xenografts by treatment with VB4-845 monotherapy nor combination therapy (Figs. 4c, d). None of the treated mice showed signs of wasting or other toxicity relative to control mice.

As shown in Figs. 5a, b of HuH-7 orthotopic xenograft model, the combined therapy of VB4-845 and 5-FU significantly suppressed the liver tumors in all mice (141 ± 34 mm^3) compared with the control (1964 ± 367 mm^3) ($p = 0.011$). The immunohistological expression of EpCAM (Fig. 5c) demonstrated that the population of strongly-stained tumor cells was decreased in VB4-845 plus 5-FU group (47.4 ± 19.4 %) compared with the control group (76.7 ± 6 %; Fig. 5d, $p = 0.012$). None of the treated mice showed signs of wasting or other toxicity relative to control mice. All host tissues examined, including liver, bone marrow, kidney, intestine, and lung, were histologically normal in all experiments.

DISCUSSION

In this study, our FACS analysis of EpCAM expression revealed that eight human HCC cell lines were classified

into two groups: four $EpCAM^{high}$ (>95 %) and four $EpCAM^{low}$ (<5 %) HCC (Fig. 1a). This is supported by the fact that VB4-845 was exceedingly effective against $EpCAM^{high}$ cell lines but not $EpCAM^{low}$ cell lines (Figs. 1b, d). Because the close correlation between EpCAM expression and sphere-formation was reported in HCC cells, we assessed the effect of VB4-845 on sphere-forming ability.[11] Although 5-FU treatment did not affect the sphere formation, the treatment with VB4-845 as well as the combination of VB4-845 plus 5-FU clearly suppressed the sphere formation in all four HCC cell lines (Figs. 2a, b; $p < 0.001$). Because the sphere-forming ability is known to be regulated by the self-renewing capacity of stem cells, the effects of VB4-845 might be closely associated with the stemness of $EpCAM^{high}$ HCC cells.[25,29]

For further investigation of the VB4-845 effects on the stemness, the expression of several stem/progenitor markers was analyzed after the treatment of VB4-845 and/or 5-FU. 5-FU treatment significantly increased the positive rates of CD133 in threeHCC cell lines (Fig. 3b; $p < 0.05$). Ma et al.[30] reported that $CD133^+$ subpopulation in HCC cells was more resistant to 5-FU than $CD133^-$ subpopulation, suggesting the $CD133^+$ subpopulation might contribute to the chemoresistance of HCC. Furthermore, VB4-845 dramatically decreased the $CD133^+$ subpopulations in these HCC cells (Fig. 3b; $p < 0.005$). Similar results were obtained from the analysis of CD13. The positive rates of CD13 were significantly decreased by VB4-845 treatment but increased by 5-FU treatment (Fig. 3c). These results indicated that the targeted subpopulations were different between the VB4-845 and 5-FU treatments. With respect to the stem/progenitor markers, the effects of VB4-845 also were found to be closely associated with the stemness of human HCC cells.

Because in vitro cytotoxic effects of VB4-845 and/or 5-FU were observed with or without apoptosis (Fig. 1d and Supplementary Fig. 2), in vivo antitumor effects were analyzed using the subcutaneous xenograft model (Fig. 4). Whereas a statistically significant antitumor effect was not detected by either VB4-845 or 5-FU monotherapy, the combination therapy of VB4-845 and 5-FU significantly decreased the exotopic tumors of $EpCAM^{high}$ HCC ($p < 0.05$). Because the organ microenvironment in cancer might play a critical role in drug sensitivity, particularly for HCC, an organotropic cancer, a liver orthotopic xenograft model having similarity with the clinical condition also was utilized to explore tumor growth inhibition.[31] As observed in the subcutaneous xenograft model, significant regression of tumors was observed in the VB4-845 plus 5-FU treated group compared with the control group (Figs. 5a, b; $p = 0.0011$).

We have previously reported that the EpCAM expression was significantly associated with poor prognosis of the patients with in CM-type HCC.[17] Indeed, our preliminary prospective study validated EpCAM as the predictive biomarker of the patient prognosis ($p = 0.0447$) as well as the recurrence (Supplementary Fig. 3, $p = 0.0171$). Other clinical studies indicated that EpCAM was one of the biomarkers of chemoresistance in HCC. Noda et al.[32] reported the correlation between the EpCAM expression and chemoresistance to interferon-α/5-FU combination therapy for HCC. In another report, the expression of EpCAM and CD133 in chemoembolized HCC tumor cells was significantly correlated with the HCC recurrence after liver transplantation.[33] These findings indicate the cancer cells expressing EpCAM could be an important target in the treatment of refractory HCC.

In our studies of VB4-845, the EpCAM-targeted therapy appears to demonstrate anticancer effects via potentially different mechanism (e.g., stemness) from the conventional cytotoxic agent 5-FU. Indeed, our preclinical studies intimate that the combination therapy of an immunotoxin targeting EpCAM with a conventional cytotoxic agent is a promising novel approach for the treatment of human HCC. Further studies and clinical trials of EpCAM-targeting agents will confirm its therapeutic role in the HCC management.

ACKNOWLEDGMENT This work was supported by Grant-in-Aid for Scientific Research on Innovative Areas, Scientific Research (A), Project of Development of Innovative Research on Cancer Therapeutics from Ministry of Education, Culture, Sports, Science & Technology of Japan, and Health & Labour Sciences Research Grant from Ministry of Health Labour & Welfare of Japan. The authors thank Dr. Glen C. MacDonald and Dr. Joycelyn Entwistle at Viventia Biotechnologies Inc. (Winnipeg, Manitoba Canada) for providing VB4-845 (Oportuzumab monatox) and manuscript review, and Ms. Ayumi Shioya for technical assistance.

GRANT SUPPORT This work was supported by Grant-in-Aid for Scientific Research on Innovative Areas, Scientific Research (A) from Ministry of Education, Culture, Sports, Science & Technology of Japan, and Health & Labour Sciences Research Grant from Ministry of Health Labour & Welfare of Japan.

CONFLICT OF INTEREST The authors declare no competing financial interests.

DISCLOSURES The authors disclose no conflicts.

REFERENCES

1. El-Serag HB. Hepatocellular carcinoma. *N Engl J Med.* 2011;365:1118–27.
2. Bruix J, Sherman M. Management of hepatocellular carcinoma: an update. *Hepatology.* 2011;53:1020–2.
3. Arii S, Sata M, Sakamoto M, et al. Management of hepatocellular carcinoma: Report of Consensus Meeting in the 45th. Annual

Meeting of the Japan Society of Hepatology (2009). *Hepatol Res.* 2010;40:667–85.
4. Llovet JM, Ricci S, Mazzaferro V, et al. Sorafenib in advanced hepatocellular carcinoma. *N Engl J Med.* 2008;359:378–90.
5. Pawlik TM, Reyes DK, Cosgrove D, Kamel IR, Bhagat N, Geschwind JF. Phase II trial of sorafenib combined with concurrent transarterial chemoembolization with drug-eluting beads for hepatocellular carcinoma. *J Clin Oncol.* 2011;29:3960–7.
6. Ben-Porath I, Thomson MW, Carey VJ, et al. An embryonic stem cell-like gene expression signature in poorly differentiated aggressive human tumors. *Nat Genet.* 2008;40:499–507.
7. Yamashita T, Forgues M, Wang W, et al. EpCAM and alpha-fetoprotein expression defines novel prognostic subtypes of hepatocellular carcinoma. *Cancer Res.* 2008;68:1451–61.
8. Yu XH, Xu LB, Liu C, Zhang R, Wang J. Clinicopathological characteristics of 20 cases of hepatocellular carcinoma with bile duct tumor thrombi. *Dig Dis Sci.* 2011;56:252–9.
9. Yang XR, Xu Y, Yu B, et al. High expression levels of putative hepatic stem/progenitor cell biomarkers related to tumour angiogenesis and poor prognosis of hepatocellular carcinoma. *Gut.* 2010;59:953–62.
10. Lu JW, Chang JG, Yeh KT, Chen RM, Tsai JJ, Hu RM. Overexpression of Thy1/CD90 in human hepatocellular carcinoma is associated with HBV infection and poor prognosis. *Acta Histochem.* 2011;113:833–8.
11. Yamashita T, Ji J, Budhu A, et al. EpCAM-positive hepatocellular carcinoma cells are tumor-initiating cells with hepatic stem/progenitor cell features. *Gastroenterology.* 2009;136:1012–24.
12. Kimura O, Takahashi T, Ishii N, et al. Characterization of the epithelial cell adhesion molecule (EpCAM)+ cell population in hepatocellular carcinoma cell lines. *Cancer Sci.* 2010;101:2145–55.
13. Ma S, Lee TK, Zheng BJ, Chan KW, Guan XY. CD133+ HCC cancer stem cells confer chemoresistance by preferential expression of the Akt/PKB survival pathway. *Oncogene.* 2008;27:1749–58.
14. Nagano H, Ishii H, Marubashi S, et al. Novel therapeutic target for cancer stem cells in hepatocellular carcinoma. *J Hepatobiliary Pancreat Sci.* 2012;19:600–5.
15. Zhu Z, Hao X, Yan M, et al. Cancer stem/progenitor cells are highly enriched in CD133+ CD44+ population in hepatocellular carcinoma. *Int J Cancer.* 2010;126:2067–78.
16. Yang ZF, Ho DW, Ng MN, et al. Significance of CD90+ cancer stem cells in human liver cancer. *Cancer Cell.* 2008;13:153–66.
17. Murakata A, Tanaka S, Mogushi K, et al. Gene expression signature of the gross morphology in hepatocellular carcinoma. *Ann Surg.* 2011;253:94–100.
18. Hui AM, Takayama T, Sano K, et al. Predictive value of gross classification of hepatocellular carcinoma on recurrence and survival after hepatectomy. *J Hepatol.* 2000;33:975–9.
19. Shimada M, Rikimaru T, Hamatsu T, et al. The role of macroscopic classification in nodular-type hepatocellular carcinoma. *Am J Surg.* 2001;182:177–82.
20. Di Paolo C, Willuda J, Kubetzko S, et al. A recombinant immunotoxin derived from a humanized epithelial cell adhesion molecule-specific single-chain antibody fragment has potent and selective antitumor activity. *Clin Cancer Res.* 2003;9:2837–48.
21. MacDonald GC, Rasamoelisolo M, Entwistle J, et al. A phase I clinical study of intratumorally administered VB4-845, an anti-epithelial cell adhesion molecule recombinant fusion protein, in patients with squamous cell carcinoma of the head and neck. *Med Oncol.* 2009;26:257–64.
22. Kowalski M, Guindon J, Brazas L, et al. A phase II study of oportuzumab monatox: an immunotoxin therapy for patients with noninvasive urothelial carcinoma in situ previously treated with bacillus Calmette-Guérin. *J Urol.* 2012;188:1712–8.
23. Aihara A, Tanaka S, Yasen M, et al. The selective Aurora B kinase inhibitor AZD1152 as a novel treatment for hepatocellular carcinoma. *J Hepatol.* 2010;52:63–71.
24. Adikrisna R, Tanaka S, Muramatsu S, et al. Identification of pancreatic cancer stem cells and selective toxicity of chemotherapeutic agents. *Gastroenterology.* 2012;143:234–45.
25. Chojnacki A, Weiss S. Production of neurons, astrocytes and oligodendrocytes from mammalian CNS stem cells. *Nat Protoc.* 2008;3:935–40.
26. Muramatsu S, Tanaka S, Mogushi K, et al. Visualization of stem cell features in human hepatocellular carcinoma reveals in vivo significance of tumor-host interaction and clinical course. *Hepatology.* 2013;58(1):218–28.
27. Tanaka S, Sugimachi K, Yamashita Yi Y, et al. Tie2 vascular endothelial receptor expression and function in hepatocellular carcinoma. *Hepatology.* 2002;35:861–7.
28. Wang Y, Sun Z, Peng J, Zhan L. Bioluminescent imaging of hepatocellular carcinoma in live mice. *Biotechnol Lett.* 2007;29:1665–70.
29. Reya T, Morrison SJ, Clarke MF, Weissman IL. Stem cells, cancer, and cancer stem cells. *Nature.* 2001;414:105–11.
30. Ma S, Lee TK, Zheng BJ, Chan KW, Guan XY. CD133+ HCC cancer stem cells confer chemoresistance by preferential expression of the Akt/PKB survival pathway. *Oncogene.* 2008;27:1749–58.
31. Tredan O, Galmarini CM, Patel K, Tannock IF. Drug resistance and the solid tumor microenvironment. *J Natl Cancer Inst.* 2007;99: 1441–54.
32. Noda T, Nagano H, Takemasa I, et al. Activation of Wnt/beta-catenin signaling pathway induces chemoresistance to interferon-alpha/5-fluorouracil combination therapy for hepatocellular carcinoma. *Br J Cancer.* 2009;100:1647–58.
33. Zeng Z, Ren J, O Neil M, et al. Impact of stem cell marker expression on recurrence of TACE-treated hepatocellular carcinoma post liver transplantation. *BMC Cancer.* 2012;12:584–94.
34. Puisieux A, Galvin K, Troalen F, Bressac B, Marcais C, Galun E, Ponchel F, Yakicier C, Ji J, Ozturk M. Retinoblastoma and p53 tumor suppressor genes in human hepatoma cell lines. *FASEB J.* 1993;7(14):1407–13.

Ann Surg Oncol
DOI 10.1245/s10434-014-4292-3

Annals of
SURGICAL ONCOLOGY
OFFICIAL JOURNAL OF THE SOCIETY OF SURGICAL ONCOLOGY

ORIGINAL ARTICLE – HEPATOBILIARY TUMORS

A Novel Therapeutic Combination Sequentially Targeting Aurora B and Bcl-xL in Hepatocellular Carcinoma

Hiroko Matsunaga, MD[1], Shinji Tanaka, MD, PhD, FACS[2], Arihiro Aihara, MD, PhD[1], Kousuke Ogawa, MD, PhD[1], Satoshi Matsumura, MD, PhD[1], Daisuke Ban, MD, PhD[1], Takanori Ochiai, MD, PhD[1], Takumi Irie, MD, PhD[1], Atsushi Kudo, MD, PhD[1], Noriaki Nakamura, MD, PhD[1], Shigeki Arii, MD, PhD[1], and Minoru Tanabe, MD, PhD[1]

[1]Department of Hepato-Biliary-Pancreatic Surgery, Graduate School of Medicine, Tokyo Medical and Dental University, Tokyo, Japan; [2]Department of Molecular Oncology, Graduate School of Medicine, Tokyo Medical and Dental University, Tokyo, Japan

ABSTRACT

Background. Effective therapeutic combinations targeting the oncogenic pathway still are unknown in human hepatocellular carcinoma (HCC). The authors previously identified aberrant expression of aurora B kinase as the independent predictor for the lethal recurrence of HCC, showing that AZD1152 induced in vitro and in vivo apoptosis with polyploidy in human HCC cells. In this preclinical study, the combined effects of molecular-targeted therapies were evaluated based on the cellular response of aurora B inhibition.

Methods. This study analyzed the expression of Bcl-2 family proteins in polyploidization induced by AZD1152 and the in vitro synergistic effects of AZD1152 with control of the Bcl-2 family pathway in human HCC cells. The in vivo effects of the combination therapy targeting the specific molecules were evaluated using subcutaneous tumor xenograft models.

Results. The findings showed that Bcl-xL was specifically overexpressed in AZD1152-induced polyploid HCC cells. The combination of AZD1152 followed by Bcl-xL/2 inhibitor ABT263 induced synergistically cellular apoptosis ($p < 0.001$) and growth inhibition ($p < 0.0001$). Interestingly, the reverse sequential administration of AZD1152 combined with pretreatment of ABT263 was less effective than the original one. In vivo studies using tumor xenografts of human HCC cells showed that combination therapy of ABT263 after AZD1152 pretreatment induced significant intratumoral apoptosis ($p < 0.05$) and remarkable anti-tumor effects ($p < 0.05$) without a severe adverse effect compared with the monotherapy.

Conclusion. Based on Bcl-xL overexpression in polyploidy induced by aurora B inhibition, the rationale for therapeutic combinations targeting aurora B and Bcl-xL was demonstrated in the authors' preclinical studies, leading to a promising novel approach for the mechanism-based treatment of human HCC.

Hepatocellular carcinoma (HCC) is one of the most common causes of cancer-related death in the world.[1] Surgical resection is considered the primary curative treatment for HCC. A major obstacle to the treatment of HCC is the high frequency of tumor recurrence even after curative resection.[2,3] According to our previous studies of HCC,[4] the aggressive recurrence showed extremely poor prognosis for the postoperative patients. Systemic chemotherapy using conventional anticancer agents has provided little clinical benefit or prolonged survival for patients with advanced HCC.[5] The recent achievement could show that molecular-targeted therapies are effective for various malignancies.[6,7] Indeed, a multikinase inhibitor, sorafenib, is reported to be the first agent to demonstrate an improved overall survival for HCC patients.[8] To fulfil this promise, there is an urgent need to identify the optimal targets for the treatment of aggressive HCC.[9–11]

Electronic supplementary material The online version of this article (doi:10.1245/s10434-014-4292-3) contains supplementary material, which is available to authorized users.

First Received: 9 October 2014

S. Tanaka, MD, PhD, FACS
e-mail: tanaka.monc@tmd.ac.jp

Published online: 19 December 2014

In our previous studies, a genome-wide microarray analysis identified an aurora B kinase as the only independent factor to predict the aggressive recurrence of HCC,[12] and the anticancer effects of aurora B inhibitor AZD1152 were demonstrated in human HCC cells.[13] Aberrant expression of the aurora B kinase has been reported in a variety of solid tumors including prostate, colon, pancreas, lung tumors.[14]

Aurora B is a chromosomal passenger serine/threonine protein kinase that regulates accurate chromosomal segregation, cytokinesis, protein localization to the centromere and kinetochore, correct microtubule–kinetochore attachments, and regulation of the mitotic checkpoint.[15] In cancer cells, inhibition of aurora B kinase results in abrogation of chromosome alignment, segregation, and also cytokinesis directly. By overriding the spindle checkpoint, these cancer cells progress into aberrant mitosis without cytokinesis, resulting in massive polyploidy and subsequent cell death.[16,17]

Reports have shown that Bcl-2 proteins control a crucial checkpoint of cellular survival during polyploidization.[18–20] The Bcl-2 family of proteins is divided into two types: anti-apoptotic proteins (Bcl-2, Bcl-xL, and Mcl-1) and pro-apoptotic proteins (Bax, Bid, Bim, and Puma).[21] The major function of the Bcl-2 family is to modulate mitochondrial membrane permeability directly and thereby regulate the release of apoptogenic factors from the intermembrane space into the cytoplasm.[21] Mitotic catastrophe after polyploidization is characterized by the activation of mitochondrial membrane permeabilization associated with the Bcl-2 family.[22] Additionally, recent studies have indicated a critical role of the Bcl-2 family of proteins in synthetic lethality with oncogene addiction for the combination therapy.[23,24]

In the current study using polyploidized HCC cells in response to aurora B inhibitor AZD1152, we identified overexpression of the anti-apoptotic protein of the Bcl-2 family. In vitro administration of the Bcl-xL/2 inhibitor ABT263 combined with AZD1152 pretreatment induced the synergistic apoptosis, and the in vivo combination of AZD1152 and ABT263 treatments had significant anti-tumor effects on xenografts of human HCC cells. Our preclinical investigation suggested that the combined therapy with aurora B and Bcl-2/xL inhibitors may offer a novel and promising approach for the treatment of HCC with a poorer prognosis.

MATERIALS AND METHODS

Reagents

For this study, AZD1152-HQPA and its prodrug AZD1152 were provided by AstraZeneca Pharmaceuticals (Macclesfield, UK), and ABT263 (Navitoclax) was purchased from Selleck Biotechnology (Houston, TX, USA).

Cell Cultures

Human HCC cell lines HLF, HLE, HuH7, and SK-Hep1 were obtained from the Human Science Research Resources Bank (Osaka, Japan) and the American Type Culture Collection (Manassas, VA, USA). The culture media were Dulbecco modified Eagle medium (DMEM; Invitrogen, Carlsbad, CA, USA) (HLF and HLE) or RPMI-1640 (Invitrogen) (SK-Hep1 and HuH7) supplemented with 5 % fetal bovine serum (FBS; Sigma, St. Louis, MO, USA) for the HLF cells or 10 % FBS for the remaining cell lines. All media were supplemented with 1 % Pen/Strep (Sigma). All cell lines were cultivated in a humidified incubator at 37 °C in 5 % carbon dioxide and collected with 0.05 % trypsin-0.03 % ethylenediaminetetraacetic acid (EDTA).

Immunocytochemistry

The immunocytochemical analysis was performed with cultured HLF cells on glass slides coated with saline in the presence of concentrated AZD1152-HQPA (100 nmol) for 72 h. These detailed methods are further described in Supplementary Methods.

Western Blotting Analysis for the Bcl-2 Family

The expression of Bcl-2 family proteins was detected by Western blotting analysis. After extraction of protein from each cell line and loading on 8–15 % sodium dodecyl sulfate–polyacrylamide gel electrophoresis, the blots were incubated overnight at 4 °C with the primary antibody as previously described.[25] We used the antibodies for Bcl-xL, Bcl-2, Mcl-1, Bax, Bid, Bim, and Puma (1:1,000; Cell Signaling Technology, Beverly, MA, USA, Catalog nos. 9941 and 9942), or anti-α-tubulin (1:5,000; Sigma, Catalog no. T9026). The appropriate secondary antibodies were added for 1 h, and the protein expression was visualized with enhanced chemiluminescence (ECL) by the ECL Western blot testing detection system (GE Healthcare,, Buckinghamshire, UK).

Time-Lapse Analysis

See Supplementary Methods for details.

Apoptosis Assay

See Supplementary Methods for details.

In Vitro Assay of Cell Proliferation and Viability

See Supplementary Methods for details.

In Vivo Studies with a Subcutaneous Tumor Xenograft Model

Female NOD.CB17-PRkdc$_{SCID}$/J 4-week-old mice were purchased from Charles River Japan Inc. (Kanagawa, Japan) and kept under pathogen-free conditions, fed standard food, and given free access to sterilized water. With the mice under anesthesia, 1×10^7 HLF or HuH7 cells were mixed with Matrigel (BD Biosciences, San Jose, CA, USA) and injected subcutaneously into both flanks. Tumor size was measured using calipers as frequently as every day, and tumor volumes were calculated as $AB^2 \times 0.5$ (A, length; B, width). After tumor formation was confirmed (100–150 mm^3; day 0), the mice were treated with AZD1132 (100 mg/kg/day, administered intraperitoneally) or control buffer for 3 consecutive days, followed by ABT263 (7 mg/kg/day, administered orally) or control buffer for 10 days. The Animal Care Committee of Tokyo Medical and Dental University School of Medicine approved the experimental protocols in accordance with its institutional guidelines (Permission #0140198C2).

Immunohistochemistry

The immunohistochemical analysis was performed on xenograft tumor tissue, which was harvested, formalin fixed, and paraffin embedded. The primary antibodies were used at the following diluted concentration in phosphate-buffered saline (PBS) containing 1 % bovine serum albumin (BSA): anti-cleaved caspase-3 (1:200; Cell Signaling Technology). The tissue sections were stained by an automated immunostainer (Ventana XT System; Ventana Medical Systems, Tucson, AZ, USA) using heat-induced epitope retrieval and a standard DAB detection kit (Ventana). The immunostaining was evaluated quantitatively by counting at least 200 cells in three different random fields (200× magnification) under a light microscope by three independent investigators. The mean value was calculated for the final result of each case.

Statistical Analysis

Experimental data are expressed as mean values with 95 % confidence intervals (CI). All p values lower than 0.05 were considered to have statistical significance. All statistical analyses were performed using SPSS version 17.0 (IBM SPSS, Chicago, IL, USA).

RESULTS

Bcl-xL Expression During Polyploidization in Human HCC Cells Treated With Aurora B Inhibitor AZD1152

In our previous studies,[12] HLF human HCC cells demonstrated relatively low sensitivity to aurora B inhibitor AZD1152. First, the expression of anti-apoptotic proteins of the Bcl-2 family (Bcl-2 and Bcl-xL) was evaluated during AZD1152-mediated polyploidization in HLF cells (100 nmol). Immunocytochemical analysis showed that Bcl-xL expression was clearly recognized in the polyploid cells after AZD1152 treatment for 72 h (85.0 ± 4.5 %) compared with control cells (14.5 ± 0.7 %; $p = 0.002$; Fig. 1, Supplementary Fig. 1), but overexpression of Bcl-2 was not detected in HLF cells with or without AZD1152 treatment (Supplementary Fig. 2).

Because Bcl-xL is known to be a druggable target,[26,27] the anti-apoptotic role of Bcl-xL was further analyzed in AZD1152-mediated polyploidization in human HCC cells.

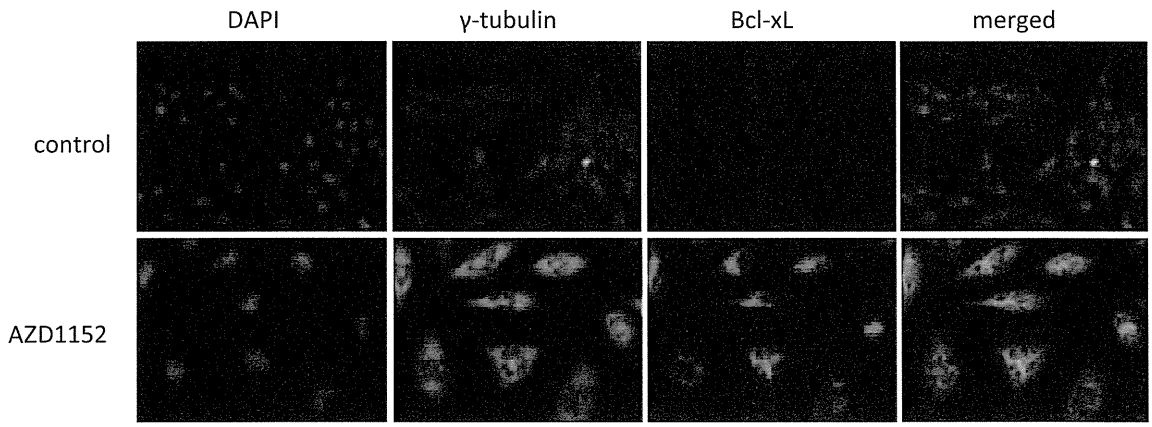

FIG. 1 Polyploidization induced by AZD1152 renders hepatocellular carcinoma (HCC) cells Bcl-xL dependent. Immunocytochemical analysis of Bcl-xL expression in HLF human HCC cells with or without AZD1152 treatment for 72 h was performed. Predominant expression of Bcl-xL was recognized in the cytoplasm of polyploid HLF cells after AZD1152 treatment (100 nmol) compared with the control cells. DAPI, 4,6-dia-midino-2-phenylindeole. Original magnification, ×200

An orally bioavailable BH3 mimetic, ABT263, which inhibits Bcl-xL and Bcl-2, was used in this study. The HLF cells were cultured for 72 h with 100 nmol of AZD1152 before being subjected to the following treatment with ABT263. After AZD1152 washout, the polyploid HLF cells were treated for 24 h with 1 μmol of ABT263 or control medium.

As shown by time-lapse analysis, ABT263 induced dominant cell death cytotoxicity in the polyploid HLF cells induced by AZD1152 (Supplementary Fig. 3a). Although a majority of AZD1152-pretreated HLF cells can survive in the control medium (87.4 ± 7.6 %), administration of ABT263 induced cytotoxicity in 84.0 ± 5.4 % of the AZD1152-pretreated HLF cells ($p < 0.0001$) (Supplementary Fig. 3b).

Significance of Anti-apoptotic Protein Bcl-xL in AZD1152-Treated HCC Cells

Next, the expression of Bcl-2 family proteins was analyzed by Western blotting on four human HCC cell lines (HLF, HLE, HuH7, and SK-Hep1) in the presence AZD1152. Among the anti-apoptotic Bcl-2 family proteins (Bcl-xL, Bcl-2, and Mcl-1), the expression of Bcl-xL was gradually increased in all the examined cell lines after AZD1152 treatment, as shown in Fig. 2a. The Bcl-2 expression was increased in AZD1152-treated SK-Hep1 cells but not in others. The expression levels of pro-apoptotic Bcl-2 family protein (Bax, Bid, Bim, and Puma) demonstrated no specific tendency to decrease or increase. Decreased expression of Bid was in HuH7 cells and slightly in HLF cells but not in others. Bim expression was decreased in SK-Hep1 cells but increased in HuH7 cells.

To evaluate the role of Bcl-xL, the cellular apoptosis was assessed by Annexin-V binding and Western blotting assays using the Bcl-xL inhibitor ABT 263 after AZD1152 pretreatment. As shown in Supplementary Figs. 4 and 5, Annexin V-positive/7-ADD-negative cells were increased in all the HCC cell lines which received the sequential combination therapy (HLF, 27.9 ± 1.7 %; HLE, 25.9 ± 0.5 %; HuH7, 25.9 ± 4.1 %; SK-Hep1, 38.4 ± 3.2 %) compared with AZD1152 monotherapy (HLF, 7.7 ± 0.2 %; HLE, 18.9 ± 2.1 %; HuH7, 18.9 ± 1.4 %; SK-Hep1, 21.1 ± 0.2 %), ABT263 monotherapy (HLF, 7.9 ± 0.5 %; HLE, 12.8 % 0.5 %; HuH7, 11.0 ± 0.5 %; SK-Hep1, 7.5 ± 1.5 %), or the control condition (HLF, 7.2 ± 0.2 %; HLE, 9.3 ± 1.0 %; HuH7, 9.3 ± 2.1 %; SK-Hep1, 2.8 ± 0.3 %). Western blotting assays confirmed the caspase-3 activation in these HCC cell lines which received the sequential combination therapy compared with the control condition (Fig. 2).

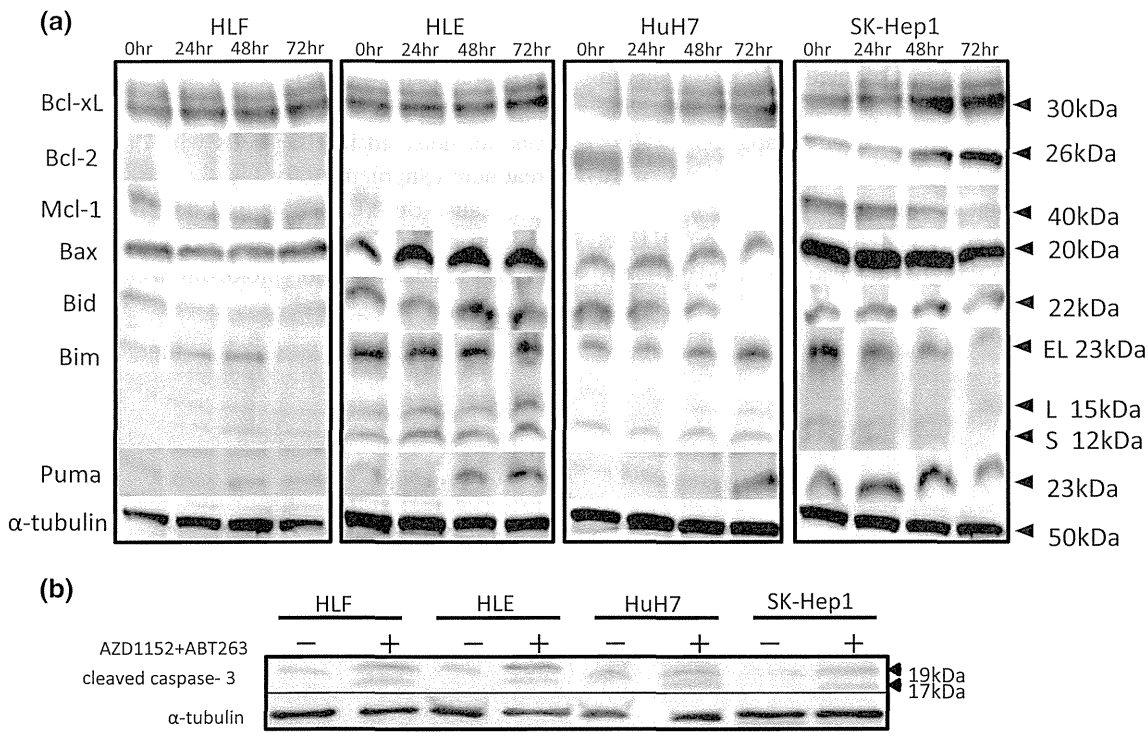

FIG. 2 Expression and anti-apoptotic role of Bcl-xL in AZD1152-treated hepatocellular carcinoma (HCC) cells (HLF, HLE, SK-Hep1, and HuH7). **a** Western blot analysis of Bcl-2 family proteins in human HCC cells treated with 100 nmol of AZD1152. Expression of anti-apoptotic proteins (Bcl-2, Bcl-xL, Mcl-1), pro-apoptotic proteins (Bax, Bid, Bim, Puma) of the Bcl-2 family, and the control alpha-tubulin was analyzed. **b** Western blot analysis of cleaved caspase-3 for detection of apoptosis in human HCC cells treated with or without sequential combination therapy using AZD1152 and ABT263

Combination with Bcl-xL Inhibitor ABT263 After Administration of AZD1152

The effect of the Bcl-xL/2 inhibitor ABT263 was evaluated in the four HCC cell lines. No significant difference in half maximal (50 %) inhibitory concentration (IC50) values of ABT263 monotherapy was recognized among these cell lines (HLF, 4.6 ± 0.3 μmol; HLE, 7.4 ± 0.5 μmol; HuH7, 6.2 ± 0.5 μmol; SK-Hep1, 11.4 ± 0.6 μmol) (Supplementary Fig. 6).

After pretreatment of various AZD1152 concentrations (0.001–1000 nmol), the synergistic effect of ABT263 (1 nmol) was then analyzed in these cell lines of human HCC. The sequential combination of AZD1152 followed by ABT263 potently inhibited the cell proliferation (HLF, 16.3 ± 0.5 nmol; HLE, 0.01 ± 0.5 nmol; HuH7, 0.2 ± 0.7 nmol; SK-Hep1, 2.3 ± 0.9 nmol) compared with AZD1152 monotherapy (HLF, 140.0 ± 1.0 nmol; HLE, 45.2 ± 0.8 nmol; HuH7, 5.7 ± 0.9 nmol; SK-Hep1, 24.4 ± 0.9 nmol; $p < 0.0001$) (Fig. 3; AZD1152 → ABT263). Additionally, the effect from reversing the sequence of AZD1152 and ABT263 administration (i.e., treating with ABT263 before AZD1152) was assessed. Some combination effect was recognized (HLF, 106 ± 2.6 nmol; HLE, 32.4 ± 0.8 nmol; HuH7, 3.3 ± 1.0 nmol; SK-Hep1, 15 ± 0.5 nmol), but statistical significance was not recognized ($p > 0.05$) (Fig. 3; ABT263 → AZD1152). Sequential combination targeting of aurora B followed by Bcl-xL treatment might indicate a therapeutic tool for human HCC.

Preclinical Studies of Combination Therapy Using Xenografts of Human HCC Cells

In vivo antitumor activity of the combination therapy for human HCC was analyzed using HLF or HuH7 subcutaneous xenografts established in nonobese diabetic/severe combined immunodeficient (NOD-SCID) mice. As shown in Fig. 4 and Supplementary Fig. 7a, a significant regression of HLF tumors was observed in the group of mice that received the sequential combination therapy compared with monotherapy (AZD1152, $p = 0.008$; ABT263, $p = 0.016$) or the control condition ($p < 0.001$). Similar antitumor effects were detected in HuH7 tumors by the sequential combination therapy compared with monotherapy (AZD1152, $p = 0.005$; ABT263, $p = 0.041$) or the control condition ($p < 0.001$; Fig. 4, Supplementary Fig. 7b). No reductions in bone marrow nucleated cells were detected at the end of the dosing period (Supplementary Fig. 8). None of the treated mice showed signs of wasting or other toxicity compared with the control mice. The combination of AZD1152 with ABT263 was tolerated at the dose at which antitumor efficacy was observed.

Pharmacobiologic Effects of Combination With AZD1152 and ABT263 on Subcutaneous Xenografts of Human HCC Cells

To investigate the pharmacobiologic effects of the combination therapy, the subcutaneous xenografts of HLF or HuH7 HCC cells were subjected to histologic analysis.

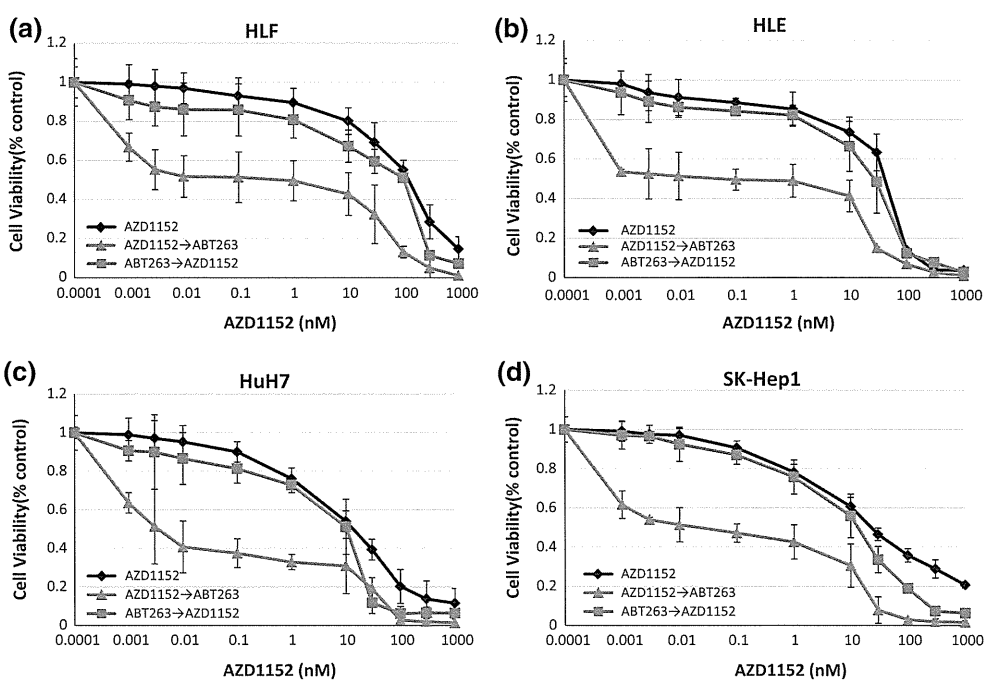

FIG. 3 Analysis of sequential combination treatment with AZD1152 and ABT263 in human hepatocellular carcinoma (HCC) cells (HLF, HLE, SK-Hep1, and HuH7). Synergistic cytotoxicity was induced by pretreatment with AZD1152 followed by posttreatment with ABT263 (AZD1152 → ABT263) but not pretreatment with ABT263 followed by posttreatment with AZD1152 (ABT263 → AZD1152) compared with AZD1152 monotherapy (AZD1152). Both AZD1152 (0.001–1000 nmol) and ABT263 (1 nmol) were used in this study

Staining of tumor samples for apoptotic marker cleaved caspase-3 showed significantly elevated levels in the sequential combination therapy of AZD1152 and ABT263 compared with AZD1152 monotherapy ($p < 0.01$), ABT263 monotherapy ($p < 0.05$), or the control condition ($p < 0.0001$) (Fig. 5). In vivo sequential combination with AZD1152 and ABT263 induced potently intratumoral apoptosis compared with the monotherapy or the control condition.

DISCUSSION

Because accumulated evidence suggests that oncogenic pathways activate the carcinogenesis and progression of cancers, many opportunities exist for the emerging development of molecular-targeted therapies, for example, inhibitors of vascular endothelial growth factor (VEGF)[28] and epidermal growth factor receptor (EGFR),[29] the mammalian target of rapamycin (mTOR),[30] and cell cycle kinases including aurora.[31,32] Based on the multiple and complex molecular pathways observed in HCCs,[33–35] several combined therapies have been attempted for HCC patients using sorafenib combined with erlotinib (EGFR inhibitor)[36] or everolimus (mTOR inhibitor)[37] and erlotinib combined with bevacizumab (VEGF inhibitor).[38] However, no sufficient effect of combined molecular-targeted therapies was recognized in these clinical trials. The rationale for targeted combinations with a molecular mechanism should be clarified in HCC.

We previously reported aurora B kinase as the unique independent predictor for the lethal recurrence of human HCC and aurora B inhibitor AZD1152 as an effective inducer of cellular apoptosis after polyploidization in human HCC cells. In the current study, we initially found that AZD1152 enhanced the expression of Bcl-xL anti-apoptotic protein in HCC cells (Figs. 1, 2). Then, combined treatment with Bcl-2/xL inhibitor ABT263 with AZD1152 was further evaluated. As shown in Supplementary Fig. 3, the synergistic killing effects of ABT263 were recognized in AZD1152-mediated polyploidy HCC cells ($p < 0.001$). The sequential combined administration of AZD1152 followed by ABT263 induced significant cytotoxicity and apoptosis in various HCC cell lines compared with either AZD1152 or ABT263 monotherapy (Fig. 3).

According to our preclinical studies (Fig. 4), in vivo combined therapy with ABT263 after AZD1152 pretreatment resulted in synergistic anti-tumor effects on subcutaneous xenografts of human HCC cells. The pharmacobiologic studies investigating the combination of ABT263 with AZD1152 confirmed in vivo induction of cellular apoptosis of human HCC cells. The combination of ABT263 with AZD1152 was well tolerated at the dose required to elicit a potent and durable anti-tumor effect in mice. According to the previous report by Rudin et al.,[39] ABT263 has induced thrombocytopenia in a dose-dependent manner, but we could not find any reductions in bone marrow nucleated cells at the end of the dosing period. Thus, the combination of Bcl-xL inhibitor with aurora B inhibitor is a promising novel therapeutic approach for the treatment of human HCC at doses that, at least preclinically, are modest and well tolerated.

As hypothesized by Weinstein and Joe,[40] cancer cells may addict a variety of oncogenic pathways for their proliferation and survival, providing a rationale for molecular-targeted therapy. But, cancers can escape from a given state

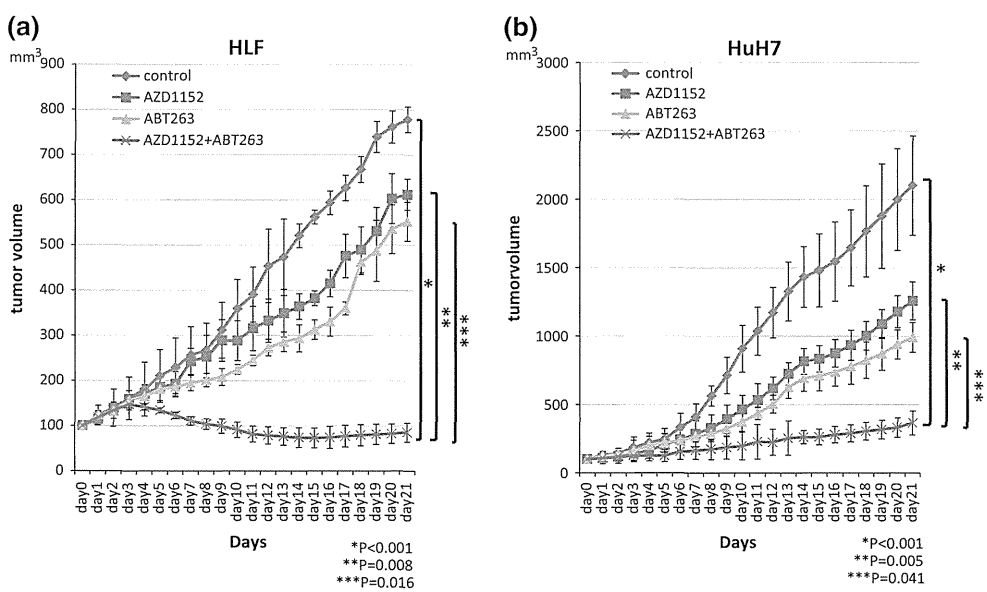

FIG. 4 In vivo effects of the sequential combination therapy with AZD1152 and ABT263 on human hepatocellular carcinoma (HCC) growth in subcutaneous xenograft models. Mice with established subcutaneous xenografts of HLF (**a**) and HuH7 (**b**) were treated with AZD1132 (100 mg/kg/day, administered intraperitoneally) or control buffer for 3 consecutive days, followed by ABT263 (7 mg/kg/day, administered orally) or control buffer for 10 days. Tumor volumes were measured everyday, and data represent mean tumor volume of five mice per treatment group

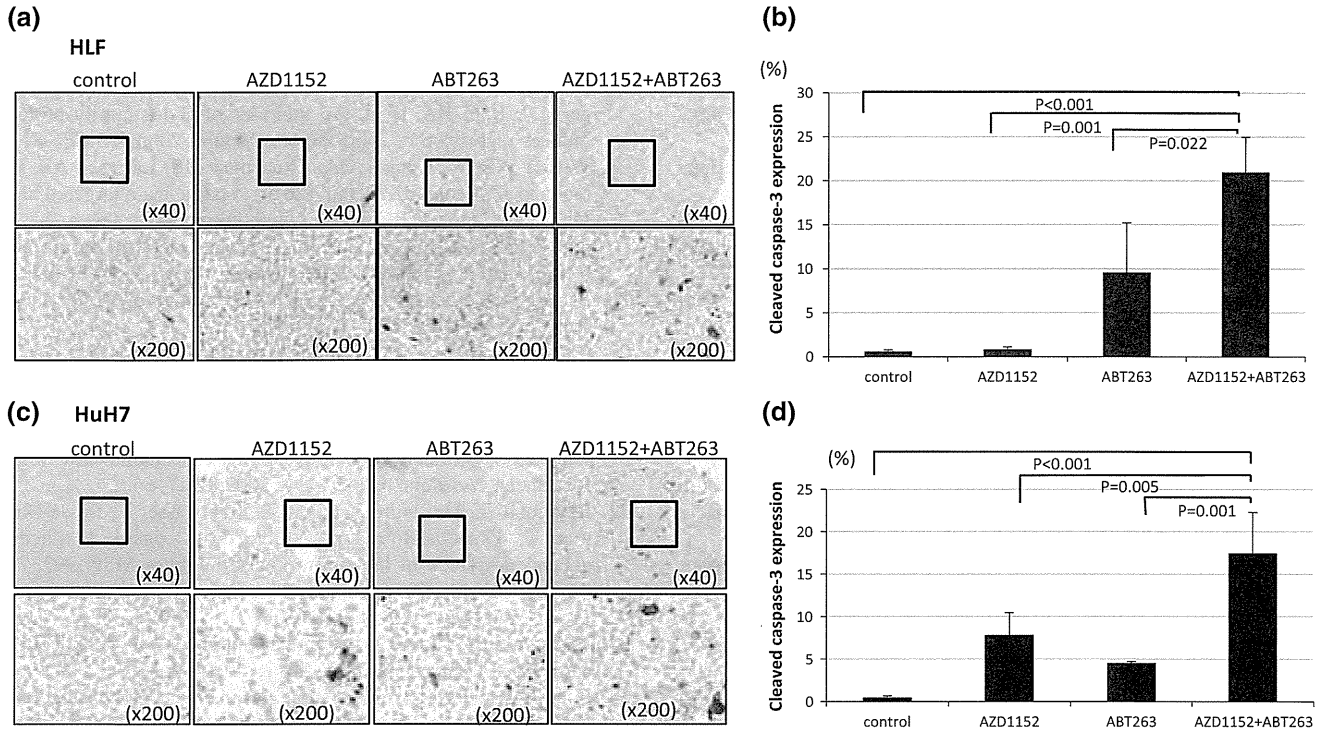

FIG. 5 Pharmacobiologic analysis of subcutaneous xenograft models. Established subcutaneous xenografts of human hepatocellular carcinoma (HCC) HLF (**a**) and HuH7 (**c**) were treated with AZD1132 (100 mg/kg/day, administered intraperitoneally) or control buffer for 3 consecutive days, followed by ABT263 (7 mg/kg/day, administered orally) or control buffer for 10 days. Transverse sections of subcutaneous tumor were analyzed for the apoptotic marker of cleaved caspase-3 (magnification, ×40 and ×200). Evaluation of the positive cell numbers per field in tumor sections of HLF (**b**) and HuH7 (**d**) HCC cells was performed. The positive cells were counted in three different random fields (magnification, ×200)

of oncogene addiction through in vitro and in vivo aberrance in other pathways and become refractory to treatment. It is unlikely that the use of a single molecular-targeted agent will achieve long-lasting remissions or cures for human cancers, especially advanced cancers. Combination therapy will therefore be required and be expected to enhance effects, not only in vitro but also in vivo.[7,41]

The current study explored the hypothesis that Bcl-xL helps to maintain the viability of polyploid cells after administration of aurora B inhibitor and concluded that the combination therapy with aurora B inhibitor followed by treatment with Bcl-xL inhibitor produced synergistic inhibition of tumor growth without significant adverse events in in vivo HCC xenograft models. In the future, our preclinical studies have indicated that the combination therapy with Bcl-xL inhibitor and aurora B inhibitor is a promising novel therapeutic approach for the treatment of human HCC by molecular-targeted combination therapy based on a molecular mechanism.

ACKNOWLEDGMENT We thank AstraZeneca for kindly providing us with AZD1152 and AZD1152-HQPA for experimental studies. We also thank Drs. Andrew Foxley and Kate Owen (AstraZeneca) for their helpful review of our manuscript. This work was supported by Grant-in-Aid for Scientific Research on Innovative Areas; Scientific Research (A) from the Ministry of Education, Culture, Sports, Science & Technology of Japan; and a Health & Labour Sciences Research Grant from the Ministry of Health Labour & Welfare of Japan.

DISCLOSURE Hiroko Matsunaga, Shinji Tanaka, Arihiro Aihara, Kousuke Ogawa, Satoshi Matsumura, Daisuke Ban, Takanori Ochiai, Takumi Irie, Atsushi Kudo, Noriaki Nakamura, Shigeki Arii and Minoru Tanabe declare that they have no conflicts of interest.

REFERENCES

1. Forner A, Llovet JM, Bruix J. Hepatocellular carcinoma. *Lancet.* 2012;379:1245–55.
2. Sherman M. Recurrence of hepatocellular carcinoma. *N Engl J Med* 2008; 359: 2045–2047.
3. Arii S, Sata M, Sakamoto S, Shimada M, Kumada T, Shiina S, et al. Managemant of hepatocellular carcinoma: report of Consensus Meeting in the 45th Annual Meeting of the Japan Society of Hepatology (2009). *Hepatol Res.* 2010;40:667–85.
4. Tanaka S, Noguchi N, Ochiai T, Kudo A, Nakamura N, Ito K, et al. Outcomes and recurrence of initially resectable hepatocellular carcinoma meeting Milan criteria: rationale for partial hepatectomy as first strategy. *J Am Coll Surg.* 2007;204:1–6.
5. Wrzesinski SH, Taddei TH, Strazzabosco M. Systemic therapy in hepatocellular carcinoma. *Clin Liver Dis.* 2011;15:423–41.
6. Sawyers C. Targeted cancer therapy. *Nature.* 2004;432:294–7.

7. Yap TA, Omlin A, de Bono JS. Development of therapeutic combinations targeting major cancer signaling pathways. *J Clin Oncol.* 2013;31:1592–605.
8. Llovet JM, Ricci S, Mazzaferro V, Hilgard P, Gane E, Blanc JF, et al. Sorafenib in advanced hepatocellular carcinoma. *N Engl J Med.* 2008;359:378–90.
9. Tanaka S, Arii S. Molecular targeted therapies in hepatocellular carcinoma. *Semin Oncol.* 2012;39:486–92.
10. Hemandez-Gea V, Toffanin S, Friedman SL, Llovet JM. Role of the microenvironment in the pathogenesis and treatment of hepatocellular carcinoma. *Gastroenterology.* 2013;114:512–27.
11. Marquardt JU, Thorgeirsson SS. SnapShot: hepatocellular Carcinoma. *Cancer Cell.* 2014;25:550–550.
12. Tanaka S, Arii S, Yasen M, Mogushi K, Su NT, Zhao C, et al. Aurora kinase B is a predictive factor for the aggressive recurrence of hepatocellular carcinoma after curative hepatectomy. *Br J Surg.* 2008;95:611–9.
13. Aihara A, Tanaka S, Yasen M, Matsumura S, Mitsunori Y, Murakata A, et al. The selective aurora B kinase inhibitor AZD1152 as a novel treatment for hepatocellular carcinoma. *J Hepatol.* 2010;52:63–71.
14. Carvajal RD, Tse A, Schwartz GK. Aurora kinases: new targets for cancer therapy. *Clin Cancer Res.* 2006;12:6869–75.
15. Ruchaud S, Carmena M, Eamshaw WC. Chromosomal passengers: conducting cell division. *Nat Rev Mol Cell Biol.* 2007;8:798–812.
16. Nicholas K, Stephen T. Aurora-kinase inhibitors as anticancer agents. *Nat Rev Cancer.* 2004;4:927–36.
17. Vogel C, Hager C, Bastians H. Mechanism of mitotic cell death induced by chemotherapy-mediated G2 checkpoint abrogation. *Cancer Res.* 2007;67:339–45.
18. Minn AJ, Boise LH, Thompson CB. Expression of Bcl-xL and loss of p53 can cooperate to overcome a cell cycle checkpoint induced by mitotic spindle damage. *Genes Dev.* 1996;10:2621–31.
19. Shen YJ, DeLong CJ, Tercé F, Kute T, Willingham MC, Pettenati MJ, Cui Z. Polyploid formation via chromosome duplication induced by CTP: phosphocholine cytidylyltransferase deficiency and Bcl-2 overexpression: identification of two novel endogenous factors. *J Histochem Cytochem.* 2005;53:725–33.
20. Shah OJ, Lin X, Li L, Huang X, Li J, Anderson MG. et al. Bcl-XL represents a druggable molecular vulnerability during aurora B inhibitor-mediated polyploidization. *Proc Natl Acad Sci USA.* 2010;107:12634–9.
21. Tsujimoto Y. Cell death regulation by the Bcl-2 protein family in the mitochondria. *J Cell Physiol.* 2003;195:158–67.
22. Casredo M, Perfettini JL, Roumier T, Andreau K, Medema R, Kroemer G, et al. Cell death by mitotic catastrophe: a molecular definition. *Oncogene.* 2004;23:2825–37.
23. Roulston A, Muller WJ, Shore GC. BIM, PUMA, and the achilles' heel of oncogene addiction. *Sci Signal.* 2013;6(268):pe12.
24. Hikita H, Takehara T, Shimizu S, Kodama T, Shigekawa M, Iwase K, et al. The Bcl-xL inhibitor, ABT-737, efficiently induces apoptosis and suppresses growth of hepatoma cells in combination with sorafenib. *Hepatology.* 2010;52:1310–21.
25. Tanaka S, Pero SC, Taguchi K, Shimada M, Mori M, Krag DN, et al. Specific peptide ligand for Grb7 signal transduction protein and pancreatic cancer metastasis. *J Natl Cancer Inst.* 2006;98:491–8.
26. Oltersdorf T, Elmore SW, Shoemaker AR, Armstrong RC, Augeri DJ, Belli BA, et al. An inhibitor of Bcl-2 family proteins induces regression of solid tumors. *Nature.* 2005;435:677–81.
27. Wilson WH, O' Connor OA, Czuczman MS, LaCasce AS, Gerecitano JF, Leonard JP, et al. (2010) Navitoclax, a targeted high-affinity inhibitor of BCL-2, in lymphoid malignancies: a phase 1 dose-escalation study of safety, pharmacokinetics, pharmacodynamics, and antitumour activity. *Lancet Oncol.* 11:1149–59.
28. Ferrara N, Gerber HP, LeCouter J. The biology of VEGF and its receptors. *Nat Med.* 2003;9:669–76.
29. Citri A, Yarden Y. EGF-ERBB signaling: towards the systems level. *Nat Rev Mol Cell Biol.* 2006;7:505–16.
30. Laplante M, Sabatini DM. mTOR signaling in growth control and disease. *Cell.* 2012;149:149–93.
31. Lapenna S, Giordano A. Cell cycle kinases as therapeutic targets for cancer. *Nat Rev Drug Discov.* 2009;8:547–66.
32. Raymond E, Alexandre J, Faivre S, Goldwasser F, Besse-Hammer T, Gianella-Borradori A, et al. A phase I schedule dependency study of the aurora kinase inhibitor MSC1992371A in combination with gemcitabine in patients with solid tumors. *Invest New Drugs.* 2014;32:94–103.
33. Villanueva A, Llovet JM. Targeted therapies for hepatocellular carcinoma. *Gastroenterology.* 2011;140:1410–26.
34. Finn RS. Emerging targeted strategies in advanced hepatocellular carcinoma. *Semin Liver Dis.* 2013;33:S11–9.
35. Lachenmayer A, Alsinet C, Chang CY, Llovet JM. Molecular approaches to treatment of hepatocellular carcinoma. *Dig Liver Dis.* 2010;42:S264–72.
36. Finn RS, Poon RT, Yau T, Klümpen HJ, Chen LT, Kang YK, et al. Phase I study investigation everolimus combined with sorafenib in patients with advanced hepatocellular carcinoma. *J Hepatol.* 2013;59:1271–7.
37. Zhu AX, Abrams TA, Miksad R, Blaszkowsky LS, Meyerhardt JA, Zheng H, et al. Phase 1/2 study of everolimus in advanced hepatocellular carcinoma. *Cancer.* 2011;15:5094–102.
38. Thomas MB, Morris JS, Chadha R, Iwasaki M, Kaur H, Lin E, et al. Phase II trial of the combination of bevacizumab and erlotinib in patients who have advanced hepatocellular carcinoma. *J Clin Oncol.* 2009;27:843–50.
39. Rudin CM, Hann CL, Garon EB, Ribeiro de Oliveira M, Bonomi PD, Camidge DR, et al. (2012) Phase II study of single-agent navitoclax ABT-263 and biomarker correlates in patients with relapsed small cell lung cancer. *Clin Cancer Res.* 18:3163–9.
40. Weinstein IB, Joe AK. Mechanisms of disease: oncogene addiction: a rationale for molecular targeting in cancer therapy. *Nat Clin Pract Oncol.* 2006;3:448–57.
41. Petricoin EF III, Bichsel VE, Calvert VS, Espina V, Winters M, Young L, et al. Mapping molecular networks using proteomics: a vision for patient-tailored combination therapy. *J Clin Oncol.* 2005;15:3614–21.

Insulin Receptor Substrate-2 (Irs2) in Endothelial Cells Plays a Crucial Role in Insulin Secretion

Short running title: Role of Irs2 in endothelial cells in insulin secretion

Shinji Hashimoto[1,*], Naoto Kubota[1,2,3,4,*], Hiroyuki Sato[1], Motohiro Sasaki[1], Iseki Takamoto[1,2], Tetsuya Kubota[1,3,4,5], Keizo Nakaya[1], Mitsuhiko Noda[6], Kohjiro Ueki[1,2], and Takashi Kadowaki[1,2,3]

[1]Department of Diabetes and Metabolic Diseases, Graduate School of Medicine, The University of Tokyo, Tokyo, Japan;
[2]Translational Systems Biology and Medicine Initiative (TSBMI), The University of Tokyo, Tokyo, Japan;
[3]Clinical Nutrition Program, National Institute of Health and Nutrition, Tokyo, Japan;
[4] Laboratory for Metabolic Homeostasis, RIKEN Center for Integrative Medical Sciences, Kanagawa, Japan;
[5]Division of Cardiovascular Medicine, Toho University Ohashi Medical Center, Tokyo, Japan;
[6]Department of Diabetes and Metabolic Medicine, International Medical Center of Japan, Toyama Hospital, Tokyo, Japan
*These authors contributed equally to this work.

Corresponding author:
Takashi Kadowaki, M.D., Ph.D. and Naoto Kubota, M.D., Ph.D.,
7-3-1 Hongo, Bunkyo-ku, Tokyo 113-8655, Japan,
Tel: 81-3-5800-8815;
Fax: 81-3-5800-9797;
E-mail: kadowaki-3im@h.u-tokyo.ac.jp (T. Kadowaki); nkubota-tky@umin.ac.jp (N. Kubota)

Word Count: 3955
Tables: 2
Figures: 6

Diabetes Publish Ahead of Print, published online October 2, 2014

Endothelial cells are considered to be essential for normal pancreatic β-cell function. The present study attempted to demonstrate the role of Irs2 in endothelial cells with regard to insulin secretion. Endothelial cell-specific insulin receptor substrate-2 knockout (ETIrs2KO) mice exhibited impaired glucose-induced, arginine-induced, and glucagon-induced insulin secretion and showed glucose intolerance. In batch incubation and perifusion experiments using isolated islets, glucose-induced insulin secretion was not significantly different between the control and the ETIrs2KO mice. In contrast, in perfusion experiments, glucose-induced insulin secretion was significantly impaired in the ETIrs2KO mice. The islet blood flow was significantly impaired in the ETIrs2KO mice. Following the treatment of these knockout mice with enalapril maleate, which improved the islet blood flow, glucose-stimulated insulin secretion was almost completely restored to levels equal to those in the control mice. These data suggest that Irs2 deletion in endothelial cells leads to a decreased islet blood flow, which may cause impaired glucose-induced insulin secretion. Thus, Irs2 in endothelial cells may serve as a novel therapeutic target for preventing and ameliorating type 2 diabetes and metabolic syndrome.

Type 2 diabetes is a heterogeneous disorder with varying degrees of insulin resistance and insulin secretion (1, 2). The United Kingdom Prospective Diabetes Study clinical trial revealed a progressive impairment in pancreatic β-cell function during the course of the disease, implicating an important role of β-cell failure in the pathogenesis of type 2 diabetes (3). Actually, the progression of type 2 diabetes is associated with minimal changes in the degree of insulin resistance; however, insulin secretion is progressively

blunted with the transition from prediabetes to overt diabetes (4). β-cell failure or dysfunction is inherently associated with type 2 diabetes and may precede the onset of hyperglycemia. Thus, the amelioration of impaired insulin secretion might be a reasonable therapeutic target.

Several studies have reported that the islet blood flow is involved in the regulation of insulin secretion. Pancreatic islets are highly vascularized by a dense network of capillaries, and various mediators, such as insulin, regulate the islet blood flow (5, 6). Iwase et al. demonstrated that orally administered insulin secretagogues acutely increased the islet blood flow (7). Moreover, renin-angiotensin system (RAS) inhibitors that regulate the islet blood flow, such as angiotensin-converting enzyme (ACE) inhibitors and angiotensin II receptor blockers (ARBs), increased insulin secretion in response to glucose administration (8-10). In addition to RAS inhibitors, some vasoactive drugs enhance pancreatic islet blood flow, augment insulin secretion and improve glucose tolerance (11, 12). These findings suggest the involvement of the islet blood flow in insulin secretion.

Irs2 is the major insulin receptor substrate isoform expressed in endothelial cells (13). We previously reported that mice with the Irs2 deletion in endothelial cells (ETIrs2KO mice) exhibited an attenuation of the insulin-induced capillary blood flow in skeletal muscle (14). In the present study, we attempted to demonstrate the relationship between insulin secretion and the islet blood flow using these mice. Although insulin secretion from isolated islets was maintained, insulin secretion was significantly impaired in the ETIrs2KO mice. These mice showed significant decreases in the islet blood flow, similar to the results seen in skeletal muscle in a previous study (14). In addition, following the administration of enalapril maleate, which enhances the islet

blood flow in these knockout mice, insulin secretion was almost completely restored to levels equal to those in the control mice. These data suggest that the absence of Irs2 in endothelial cells impairs the islet blood flow, which may be one of the mechanisms responsible for the decrease in insulin secretion. We previously reported that hyperinsulinaemia linked to obesity leads to the downregulation of Irs2 in endothelial cells (14). Thus, Irs2 in endothelial cells may serve as a novel therapeutic target for preventing and ameliorating type 2 diabetes and metabolic syndrome.

RESEARCH DESIGN AND METHODS

Animals

ETIrs2KO mice were generated as described previously (14). C57BL/6J mice were obtained from CLEA Japan (Tokyo, Japan). Mice were housed under a 12-h light-dark cycle and were given access ad libitum to normal chow MF consisting of 25% (w/w) protein, 53% carbohydrates, 6% fat and 8% water (Oriental Yeast Co., Ltd., Osaka, Japan). All the experiments in this study were performed on male mice. To evaluate the effect of an ACE inhibitor on the islet blood flow and glucose-induced insulin secretion, enalapril maleate (100 μg/kg body weight) or the corresponding volume of saline (0.1 mL) was injected intravenously. The animal care and experimental procedures were approved by the Animal Care Committee of the University of Tokyo.

Glucose tolerance test

Mice were denied access to food for 16 h starting at 19:00 hours on the previous evening and continuing until the end of the fasting period. Control and ETIrs2KO mice were intraperitoneally injected with glucose (3.0 g/kg body weight) to evaluate insulin secretion. Mice were also injected intraperitoneally with L-arginine monohydrochloride

(2.1 g/kg body weight) and glucagon (10 mg/kg body weight; Glucagon G Novo, Novo Nordisk, Bagsvaerd, Denmark). Blood samples from tail snips were collected at the indicated times, and the blood glucose level was immediately measured using an automatic blood glucose meter (Glutest Pro, Sanwa Kagaku Kenkyusho, Nagoya, Japan). Whole blood samples were collected and centrifuged in heparinized tubes, and the plasma samples were stored at -30°C. The insulin levels were determined using an insulin radioimmunoassay (RIA) kit (Institute of Isotopes, Budapest, Hungary) using rat insulin as the standard.

Assay of insulin secretion from isolated islets and of the islet insulin content

Pancreatic islets were isolated from 12 week-old mice using collagenase digestion, as described previously (15). Insulin secretion from the islets was measured under static incubation with Krebs-Ringer-bicarbonate (KRB) buffer (129 mM NaCl, 4.8 mM KCl, 1.2 mM MgSO4, 1.2 mM KH2PO4, 2.5 mM CaCl2, 5 mM NaHCO3, and 10 mM HEPES; pH7.4) containing 0.2% bovine serum albumin. In the static incubation experiments, batches of 10 freshly isolated islets were preincubated at 37°C for 30 min in 500 μL of KRB buffer containing 2.8 mM glucose. The preincubation solutions were replaced with 500 μL of KRB buffer containing the test agents, and the batches of islets were incubated at 37°C for 60 min. At the end of the incubation, aliquots of the buffer were immediately sampled and stored at -30°C until assay. For measurement of the islet insulin content, islets were solubilized in acid-ethanol solution overnight at -30°C. The insulin concentration was measured using an insulin RIA kit, and the resulting concentration was corrected according to the DNA content. The DNA content was measured using a DNA assay kit (PicoGreen, Invitrogen, Carlsbad, CA, USA).

Islet perifusion

The kinetics of insulin secretion were studied in vitro using a perifusion system. Isolated pancreatic islets were used immediately after isolation. Size-matched islets (n = 50) were placed in each column. Then, the columns were gently closed with the top adaptors and immersed in a vertical position in a temperature-controlled water bath at 37°C. The perifusion medium was maintained at 37°C in a water bath. All the columns were perifused in parallel at a flow rate of 0.6 mL/min. After 30 min of static incubation with KRB buffer (2.8 mmol/L glucose), the islets were stimulated by the continuous addition of 22.2 mmol/L of glucose. Samples were collected every 2 min and stored at -30°C until further analysis.

Quantitative reverse-transcriptase PCR

Total RNA was extracted from the islets using an RNeasy kit (QIAGEN Sciences, Maryland, USA), in accordance with the manufacturer's instructions. After treatment with RQ1 RNase-free DNase (Promega, Madison, WI) to remove genomic DNA, cDNA was synthesized using MultiScribe reverse transcriptase (Applied Biosystems, Foster City, CA), and TaqMan quantitative PCR (50°C for 2 min, 95°C for 10 min followed by 40 cycles of 95°C for 15 s, 60°C for 1 min) was then performed using the ABI Prism 7900 PCR system (Applied Biosystems) to amplify Insulin1, Insulin2 and Cyclophilin cDNA. The primers that were used were purchased from Applied Biosystems. The relative abundance of the transcripts was normalized to the constitutive expression of cyclophilin mRNA.

Histological and immunohistochemical analysis of the islets

Isolated pancreata were fixed with 4% paraformaldehyde at 4°C overnight. Tissues were routinely processed for paraffin embedding, and 4-μm sections were cut and mounted on silanized slides. Pancreatic sections were stained with anti-rabbit insulin